Available online at www.eccomasproceedia.org
Eccomas Proceedia COMPDYN (2023) 3570-3579

ECCOMAS
Proceedia

COMPDYN 2023
9th ECCOMAS Thematic Conference on
Computational Methods in Structural Dynamics and Earthquake Engineering
M. Papadrakakis, M. Fragiadakis (eds.)
Athens, Greece, 12-14 June 2023

PERMANENT DISPLACEMENT DATABASE OF STRONG EARTHQUAKES IN TURKEY, AND AN ADJUSTED PREDICTIVE MODEL

Emrecan Adanır[1] **and Gülüm Tanırcan**[1]

[1] Boğaziçi University Kandilli Observatory and Earthquake Research Institute Department of Earthquake Engineering
emrecan.adanir@boun.edu.tr, birgore@boun.edu.tr

Abstract

For seismic design and performance assessment of structures in near-fault regions, international codes recommend selecting sufficient number of strong ground motion recordings containing pulse characteristics. Permanent displacements (PD), also known as fling steps, on the other hand cannot be easily recovered from strong ground recordings because the standard filtering techniques eliminate the low- frequency portions of the motion. Recently, data processing schemes, which are based on de-trending in separate time windows, are proposed to unveil the PDs on the recordings. In this work, the data processing scheme eBASCO (Schiappapietra et al., 2021) is improved and the PDs of strong motion records calculated with new scheme is compared with GPS data of 21 worldwide earthquakes. Then, PDs in horizontal, fault normal, fault parallel and maximum direction components of Mw≥ 6 shallow crust earthquakes in Turkey are calculated to create a fling inventory for the first time. A database comprising 288 recordings ($R_{JB} \leq 50$ km) of 20 earthquakes occurred between 1983-2022 is utilized. Results are also utilized to improve the fling step prediction model of Burks and Baker (2016). Three major outcomes of this study are (1) a new comprehensive automatic data processing scheme; (2) a contribution of 22% and 33% to the fling values of normal and strike-slip earthquakes in the NESS-v2 database, respectively. Moreover, the modified processing scheme on worldwide data possibly will result in a much larger database based on our findings; (3) A Turkey-adjusted fling step predictive model.

Keywords: Permanent displacement, fling step, near fault effects, strong motion database, scaling relation, baseline correction, earthquake waveform processing.

ISSN:2623-3347
Peer-review under responsibility of the organizing committee of COMPDYN 2023.
doi: 10.7712/120123.10661.21433

1 INTRODUCTION

Directivity and fling step are distinct characteristics of near-fault strong ground motions detected as full and half cycle pulses, respectively, on the velocity waveforms. In seismic design of structures, near-fault effects are taken into consideration through site specific evaluation since they are capable of causing damages on long period structures. Seismic design codes such as International Building Code (IBC, ICBO 2006) [24] and California Building Code (CBC, ICBO 2007) [25], which are based on ASCE7-22 (ASCE 2005) [26], recommend to select strong motion records including pulse characteristics of the motions for use in nonlinear response history analysis of structures. However, due to the fact that the widely utilized data processing schemes such as filtering mask the PDs, these records cannot be identified. To overcome disadvantages of filtering, 2 methods are adopted (1) constructing an artificial fling step and superimposing it on to processed time histories (Abrahamson, 2002 [4]); (2) processing the raw records by special data processing schemes to reveal fling step (Iwan et al., 1985 [1]; Boore, 2001 [2];Wu and Wu, 2007 [6]; D'Amico et al., 2018 [11]; Schiappapietra et al., 2021 [13]).

All available proposed special data processing procedures are based on baseline correction of the waveforms. Iwan et al. (1985) [1] presented a correction algorithm which consists of the evaluation of the baseline offsets in the strongest portion of the motion and the following end part. Later, Boore (2001) [2] redefined the correction points of the former study. Wu and Wu (2007) [6] altered the former methodology so that the ground motions are separated into 3 windows; and selection of the corrected trace is connected to flatness of the last portion. D'Amico et al. (2018) [11] presented eBASCO semi-automatic processing scheme. Schiappapietra et al. (2021) [13] upgraded the eBASCO procedure in that they introduced the comparison of the acceleration amplitudes at the correction points before and after processing of the records. In this paper, eBASCO by D'Amico et al. (2018) [11] is improved to increase the number of possible combinations of correction points. Validation of the improved processing scheme is done by comparing the PDs of processed strong motion records both from Turkey and worldwide earthquakes with those derived from the co-located GPS stations. Then, by exposing the near fault ground motion records to the proposed scheme, the PD database of Turkey is created.

Next, performance of the PD predictive models of Burks and Baker (2016) [8] is evaluated through a residual analysis. It is found that Burks and Baker (2016) [8] predictive model underestimates values for small earthquakes whereas overestimates them for slightly larger earthquakes. The best estimates of this model are found for the events with magnitudes ranging between Mw 6.6 to 6.9. Burks and Baker (2016) [8] fling predictive model is then adjusted by using earthquakes in Turkey. The adjusted model is found much more effective to capture the PDs in Turkey.

2 METHODOLOGY

In this study, eBASCO data processing scheme is improved. Differences of the improved procedure from eBASCO are presented as follows:

- The first amplitude of the acceleration time history is assigned as zero to make sure that the velocity oscillates around zero at the beginning of the motion, instead of subtracting it from the whole trace.

- Energy distribution for the selecting of the time correction points is defined by normalized Arias intensity.
- The time correction points are assigned as seconds to increase the possible combinations and thus the accuracy of the obtained corrected waveform.
- Constant detrending in post-event window together with the linear detrending in other time windows shows a reliable trend that was defined as a ramp function and thus used. Conformity is provided through an additional constant baseline correction between the sample point when the strongest pulse finishes and the end.
- Instead of relying on only the acceleration amplitude comparisons, the possible erroneous spurious spikes on the obtained acceleration time history is corrected by assigning the means of the nearest acceleration amplitudes to the amplitude corresponding to time correction points [19].
- It is assumed that the ground displacement fades by oscillating around the permanent displacement level after the most of the excitation energy is dissipated. Therefore, the fade level, also known as PD, is defined as the mean of the 95% of the dissipated cumulative energy to the end of the record [20].
- In contrast to eBASCO, cut of the record in the beginning of the processing is not recommended unless it is inevitable. Moreover, the Butterworth filter at the end of the processing scheme is also not recommended to preserve the low frequency portion of the motion.

To test the capability of the proposed scheme, revealed PDs from GPS data of worldwide earthquakes are compared with the those obtained with processed records at stations in similar locations. As an example, Figure 1 illustrates the comparison of PDs of the 1999 Chi Chi earthquake station TCU 074 obtained by Yu et al (2001) [3] with those found after processing the records. Similarly, the proposed scheme is managed to capture PDs from 1 cm to 260 cm in the validation process. Comparisons of the PDs obtained from the processed records and those derived from co-located GPS data are presented with magnitudes of the events in Figure 2.

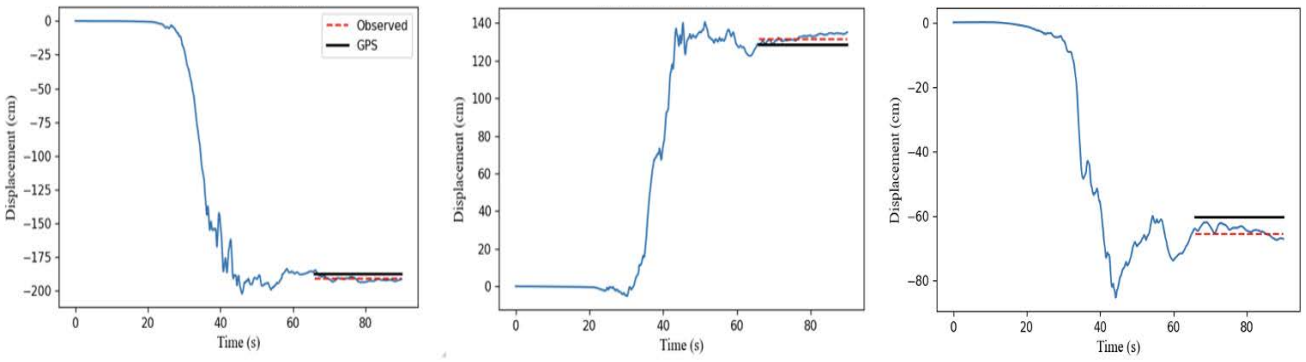

Figure 1: Displacement time history of 1999 Chi Chi earthquake EW, NS and UD components of the station TCU 074 with the findings from GPS data.

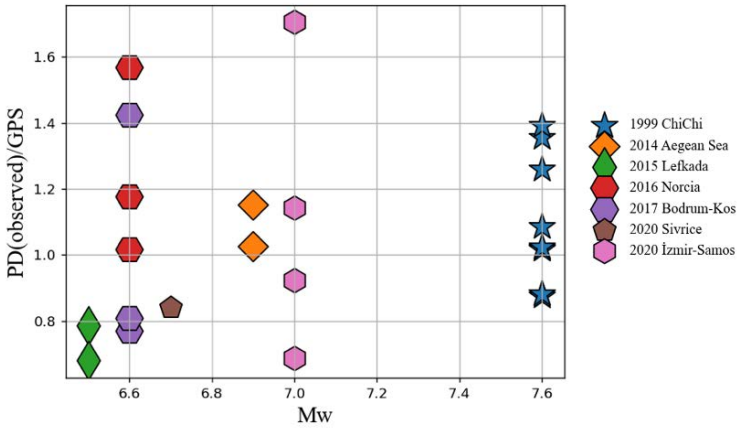

Figure 2: The comparison of PDs obtained on records with those derived from GPS

3 PERMANENT DISPLACEMENT (PD) DATABASE OF STRONG EARTHQUAKES IN TURKEY

To compile the ground motion records containing fling-steps, the new Turkish strong ground motion dataset of Turkey N-TSMD presented by Akbaş et al. (2023) [23] is utilized. Raw ground motion records are obtained from Earthquake Research Department of Disaster and Emergency Management Authority (AFAD, https://tadas.afad.gov.tr/list-waveform, last accessed December 2022) and Engineering Strong Motion Database (ESM, https://esm-db.eu/#/waveform/search, last accessed December 2022). Shallow crustal earthquakes Mw>6 and with depth <30 km have been selected. Distance limitation is set as 50 km from the surface projection of the rupture plane (R_{JB} ≤50 km). A total of 288 near-fault records, 14 strike slip, 5 normal and 1 reverse faulting earthquakes are found within the defined criteria (Figure 3). The database includes 74 records from strike slip and 81 records from normal earthquakes. Considering the fact that normal faulting earthquakes were not common in the previous studies, knowledge of the fling step occurrence in normal faulting earthquakes is increased.

Table 1: Summary of Earthquakes and Number of Data Incorporated to the study. SoF: Style of Faulting; SS: Strike Slip; N: Normal; R: Reverse; M_0: Seismic Moment

Date	SoF	Magnitude (Mw)	Number of Stations/Records	Date	SoF	Magnitude (Mw)	Number of Stations/Records
30.Oct.83	SS	6,60	1/3	1.May.03	SS	6,30	1/3
13.Mar.92	SS	6,60	1/1	8.Mar.10	SS	6,10	1/3
6.Nov.92	SS	6,00	2/6	23.Oct.11	R	7,10	1/3
1.Oct.95	N	6,10	3/7	10.Jun.12	SS	6,10	2/6
27.Jun.98	SS	6,20	1/3	24.May.14	SS	6,90	6/18
31.Jul.98	SS	6,20	6/18	12.Jun.17	N	6,30	3/9
17.Aug.99	SS	7,60	13/37	20.Jul.17	N	6,60	9/27
12.Nov.99	SS	7,10	14/42	24.Jan.20	SS	6,70	10/30
6.Jun.00	SS	6,00	1/3	30.Oct.20	N	7,00	11/33

3.Feb.02	N	6,50	1/3	23.Nov.22	SS	6,00	11/33

PDs are calculated and results in 3 orthogonal components are presented in Figure 3. The largest PD is observed in the horizontal components of TK 8101 recording during the 1999 Düzce earthquake as 263 cm and 212 cm. They are followed by 186 cm during the 1999 Kocaeli earthquake.

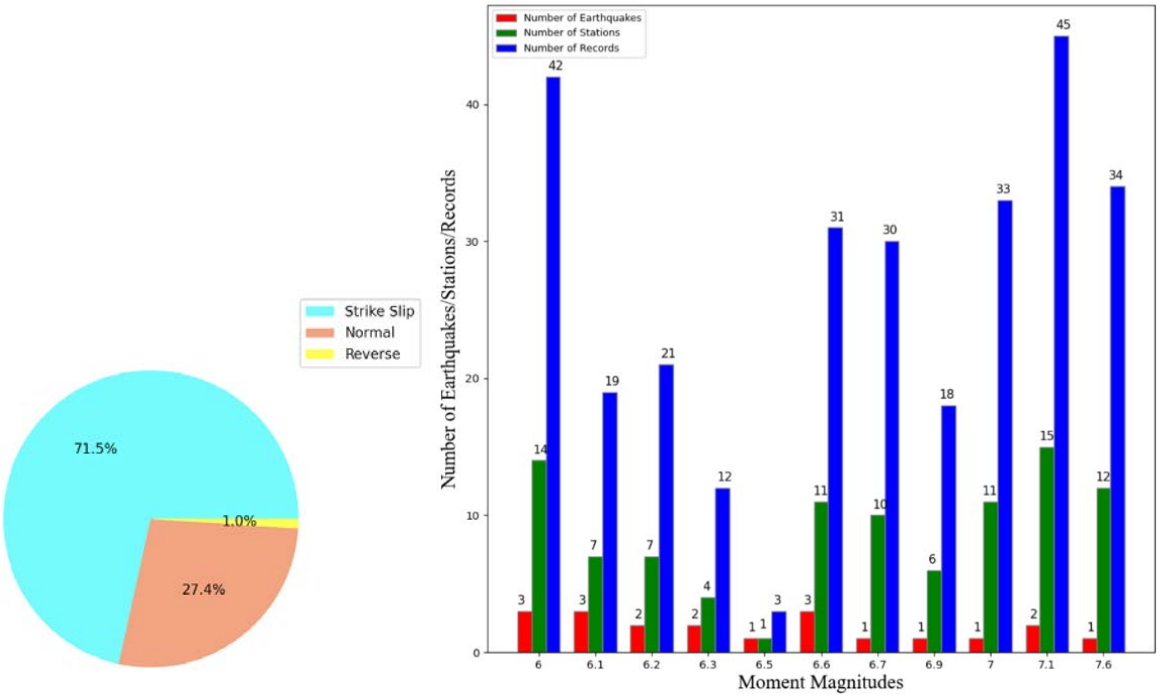

Figure 3: (Left) Distribution of the earthquakes in the dataset in terms of style of faulting (right) Distribution of the records with respect to Moment Magnitudes

As an example, resulting waveforms of the 1999 Kocaeli earthquake North-South component of YPT station and 1999 Düzce earthquake East-West component of station TK 8101 are demonstrated in Figure 4. The distribution of the PDs is illustrated in Figure 5.

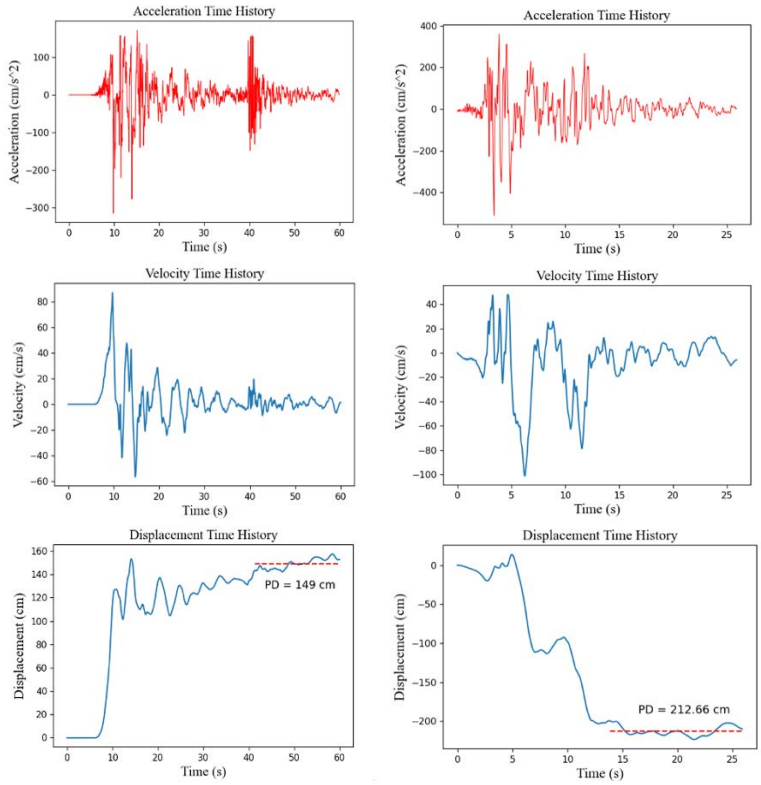

Figure 4: Processed waveforms of (left) the 1999 Kocaeli earthquake North-South component of YPT station and (right) the1999 Düzce earthquake East-West component of TK 8101 station

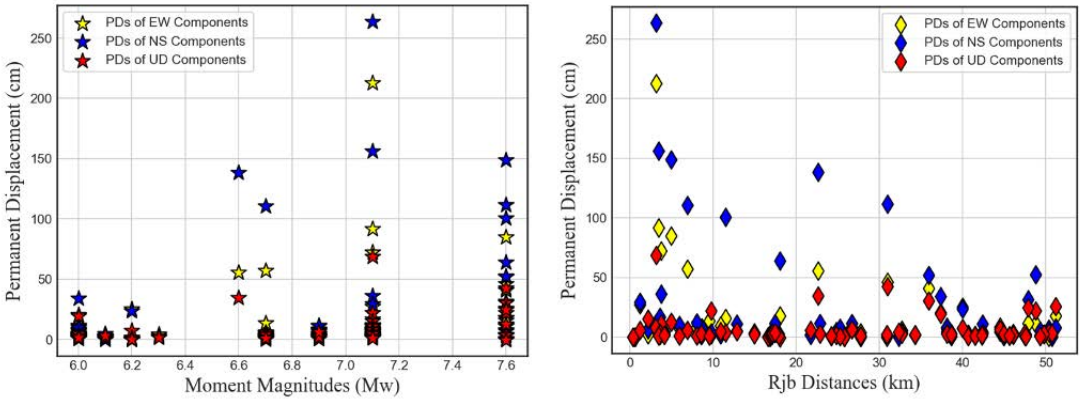

Figure 5: Distribution of the obtained PDs in EW, NS, and UD components with Mw (left) and Rrup (right)

4 EVALUATION OF PERMANENT DISPLACEMENT (PD) PREDICTION MODELS

Among several PD prediction models, Burks and Baker (2016) [8] model has been considered in this study. This model was created by inspecting the FP and FN components that obtained on kinematic and hybrid broadband earthquake simulations. Although the utilized scenario earthquakes are either strike slip or reverse faulting, Burks and Baker (2016) [8] does not depend on style of faulting as follows:

$$ln(D_p) = ln(cot^{-1}(0.3R)) + 1.3M - 5.1 \quad (1)$$

where D_p is predicted fling, R is the closest distance, Rrup, and M is moment magnitude.

Residual analyses are conducted according to Gülerce et al. (2016) [21] by considering each record (i) from each event (j) as follows:

$$R_{ij} = ln(a_{ij}) - ln(p_{ij}) = c_k + \Delta_{Bj} + \Delta_{Wij} \quad (2)$$

where R_{ij} is the total residual, a_{ij} is the PD observed on the processed record and p_{ij} is the predicted value. The total residual is divided into three parts: c_k, the average bias of the real PDs relative to predicted ones, Δ_{Bj}, inter-event residuals, and Δ_{Wj}, intra-event residuals.

With the view of engineering perspective, the calculated directions with PD≥ 3 cm are included in the residual analyses. Since the Burks and Baker (2016) [8] predictive model is based on the PDs in the slip direction of earthquake simulations, the computed values are compared with those obtained on FP components of strike slip earthquakes and FN component of normal faulting earthquakes. Figure 6 exhibits the obtained total, inter- and intra-event residuals with the Burks and Baker (2016) [8].

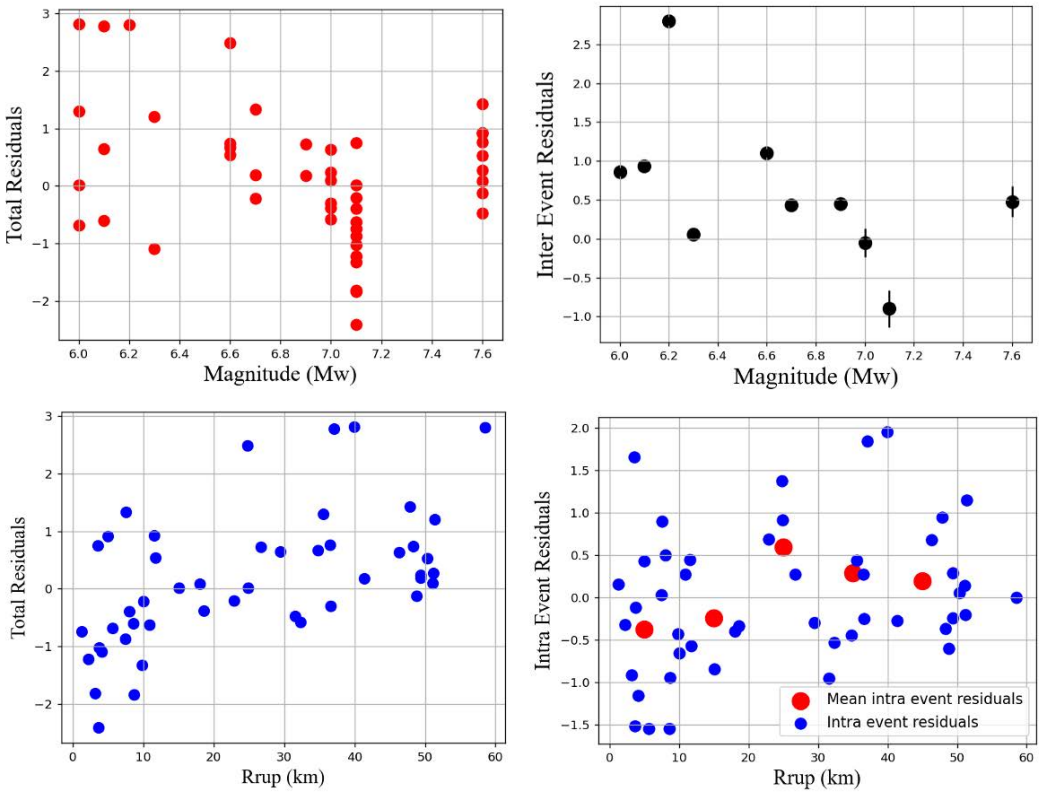

Figure 6: Distribution of (left) the total residuals of PDs with Mw and the Rrup (right) inter-event and intra-event residual distribution of PDs with Mw and the Rrup

Burks and Baker (2016) [8] is found useful to estimates the PDs to some extent. For instance, PDs of the 1999 Kocaeli (Mw 7.6) earthquakes and those of the earthquakes with magnitude ranging between Mw 6.6 to Mw 6.9 are well captured by Burks and Baker (2016) [8] predictive model. Nevertheless, in a broader sense, it is found that the model needs to be adjusted to Turkey earthquakes.

5 TURKEY ADJUSTED VERSION OF BURKS AND BAKER (2016) PD PREDICTIVE MODEL

Burks and Baker (2016) [8] model is revised with PD values of Turkish strong motion records. A random-effects regression is executed and plots of the residuals are utilized to evaluate the differences in magnitudes and distances. Modification of the predictive model is conducted by removing the observed trends on the residual graphics. First, a linear trend is found in the distribution of the inter-event residuals of the earthquakes and it is removed by incorporating in the prediction equation. Then, the intra-event residuals of the partly modified model are evaluated. It is found that in the first 10 km, the scatter of data with Rrup is quite different. Therefore, the distribution of intra event residuals are evaluated separately for the first 10 km and 10-50 km. Consecutive inter- and intra-event adjustments are defined as cycles. After 4 cycles, Turkey adjusted version of Burks and Baker (2016) [8] predictive model is obtained as:

Rrup > 10km:

$$Ln(cot^{-1}(0.3Rrup)) + 0.672Mw + 0.0113Rrup - 0.63994$$

Rrup ≤ 10km: (3)

$$Ln(cot^{-1}(0.3Rrup)) + 0.672Mw + 0.0327Rrup - 0.9847$$

Comparisons of the inter-event residuals of Burks and Baker (2016) [8] and its Turkey-adjusted version are illustrated in Figure 7. The conformity of the adjusted equation is found well.

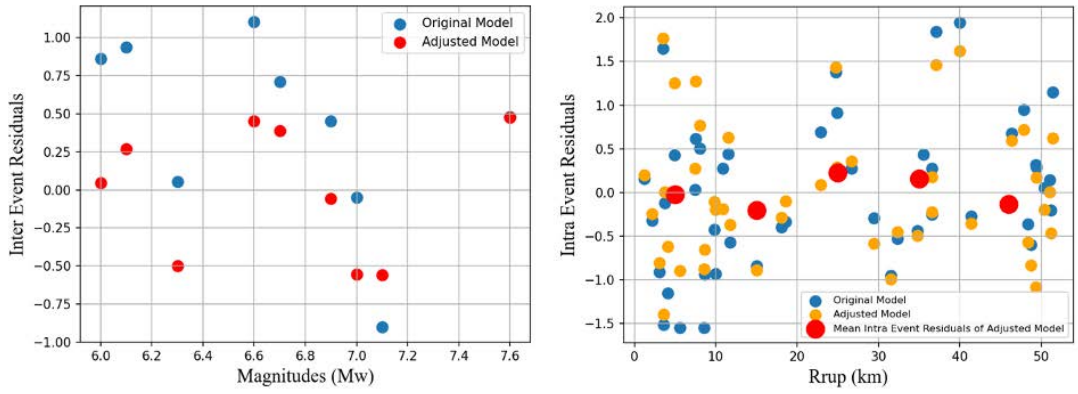

Figure 7: The comparison of the inter- and intra-event residuals of Burks and Baker (2016) and its Turkey-adjusted version

6 CONCLUSION

Near fault effects can be incorporated in seismic design of structures by selecting and scaling the actual ground motions. However, since the PD is hidden on account of the standard processing methods such as filtering the low frequency portion of the motion, there has been a need for identification of the fling containing ground motion records. In this study, an improved data processing scheme is presented. Then, by exposing the near fault records to the proposed scheme, for the first time, PD database of Turkey is compiled, which enables structural engineers to select the appropriate motions. Through the processed earthquakes in Turkey, NESS-v2 database containing the worldwide data is remarkably augmented.

In addition, obtained PDs are utilized to evaluate the performance of the Burks and Baker (2016) [8] predictive models. Due to scarcity of empirical data, prediction models are mainly based

on earthquake simulations, which is possibly the reason behind the discrepancies. Aligned with this interpretation, Burks and Baker (2016) [8] is adjusted to Turkey earthquakes by utilizing the residual plots of the created database.

ACKNOWLEDGEMENTS

This study was supported by Boğaziçi University Research Fund Grant Number 19201.

REFERENCES

[1] Iwan, W.D.; Moser, M.A.; Peng, C. Some observations on strong-motion earthquake measurement using a digital accelerograph. Bull. Seismol. Soc. Am. 1985, 75, 1225–1246.

[2] Boore DM. Effect of baseline corrections on displacements and response spectra for several recordings of the 1999 Chi-Chi, Taiwan, earthquake. Bulletin of the Seismological Society of America 2001;91(5):1199–211

[3] Yu, S.-B., L.-C. Kuo, Y.-J. Hsu, H.-H. Su, C.C. Liu, C.-S. Hou, J.-F. Lee, T.-C. Lai, C.C. Liu, C.-L. Liu, T.-F. Tseng, C.-S. Tsai, and T.-C. Shin, Preseismic deformation and coseismic displacements associated with the 1999 Chi-Chi, Taiwan, earthquake., Bulletin of the Seismological Society of America., 91 (5), 995-1012, 2001.

[4] Abrahamson NA. Velocity pulses in near-fault ground motions. In: Proceedings of the UC Berkeley - CUREE Symposium in Honor of Ray Clough and Joseph Penzien. Berkeley, California; 2002, p. 40–1.

[5] Kalkan E, Kunnath SK. Effects of fling step and forward directivity on seismic response of buildings. Earthquake Spectra 2006;22(2):367–90

[6] Wu YM, Wu CF. Approximate recovery of coseismic deformation from Taiwan strong-motion records. Journal of Seismology 2007;11:159–70.

[7] Chao, W. A., Y. M. Wu, and L. Zhao (2010). An automatic scheme for baseline correction of strong- motion records in coseismic deformation determination, J. Seismol. 14, no. 3, 495–504

[8] Burks, L. S., and J. W. Baker (2016). A predictive model for fling-step in near-fault ground motions based on recordings and simulations, Soil Dynam. Earthq. Eng. 80, 119–126, doi: 10.1016/j.soil- dyn.2015.10.010.

[9] Istituto Nazionale di Geofisica e Vulcanologia (INGV) Working Group "GPS Geodesy (GPS Data and Data Analysis Center)" (2016). Preliminary Co-seismic Displacements for the October 26 (Mw 5.9) and October 30 (Mw 6.5) Central Italy Earthquakes from the Analysis of GPS Stations, doi: 10.5281/zenodo.167959.

[10] Konca, A. O., Guvercin, S. E., Ozarpaci, S., Ozdemir, A., Funning, G. J., Dogan, U., Ergintav, S., Floyd, M., Karabulut, H., Reilinger, R., Slip distribution of the 2017 Mw6.6 Bodrum–Kos earthquake: resolving the ambiguity of fault geometry, Geophysical Journal International, Volume 219, Issue 2, November 2019, Pages 911–923, https://doi.org/10.1093/gji/ggz332

[11] D'Amico, M.; Felicetta, C.; Schiappapietra, E.; Pacor, F.; Gallovicˇ, F.; Paolucci, R.; Puglia, R.; Lanzano, G.; Sgobba, S.; Luzi, L. Fling, Effects from Near-Source Strong-Motion Records: Insights from the 2016 Mw 6.5 Norcia, Central Italy, Earthquake. Seism. Res. Lett. 2018, 90, 659–671.

[12] Konca, A. O., Cetin S., Karabulut, H., Reilinger, R., Dogan, U., Ergintav, S., Cakir, Z., Tari, E.,The 2014, MW6.9 North Aegean earthquake: seismic and geodetic evidence for coseismic slip on persistent asperities, Geophysical Journal International, Volume 213, Issue 2, May 2018, Pages 1113–1120, https://doi.org/10.1093/gji/ggy049

[13] Schiappapietra,E.; Felicetta, C.; D'Amico, M. Fling-Step Recovering from Near-Source Waveforms Database. *Geosciences* **2021**, *11*, 67. https://doi.org/ 10.3390/geosciences11020067

[14] Dogru, A., Bulut, F., Yaltirak, C., Aktug, B.,Slip distribution of the 2020 Elazığ Earthquake (Mw 6.75) and its influence on earthquake hazard in the Eastern Anatolia, Geophysical Journal International, Volume 224, Issue 1, January 2021, Pages 389–400, https://doi.org/10.1093/gji/ggaa471

[15] Aktuğ, B., Tiryakioğlu, İ., Sözbilir, H., Özener, H., Özkaymak, Ç., Yiğit, C. Ö., Softa, M. (2021). GPS derived finite source mechanism of the 30 October 2020 Samos earthquake, Mw = 6.9, in the Aegean extensional region. Turkish Journal of Earth Sciences, 30(S1), 718–737

[16] Disaster And Emergency Management Authority (1973). Turkish National Strong Motion Network [Data set]. Department of Earthquake, Disaster and Emergency Management Authority, https://doi.org/10.7914/SN/TK

[17] Engineering Strong Motion Database (ESM) (Version 2.0). Istituto Nazionale di Geofisica e Vulcanologia (INGV). https://doi.org/10.13127/ESM.2

[18] Burks, Lynne S., and Jack W. Baker. Fling in near-fault ground motions and its effect on structural collapse capacity. *Proceedings of the 10th National Conference in Earthquake Engineering*, Earthquake Engineering Research Institute, Anchorage, AK, 2014.

[19] Boore DM, Bommer JJ. Processing of strong-motion accelerograms: needs, options and consequences. *Soil Dynamics and Earthquake Engineering* 2005; **25**: 93–115.

[20] Trifunac, M. D. and Brady, A. G. (1975) A study on the duration of strong earthquake ground motion. Bulletin of the Seismological Society of America, 65 (3). pp. 581-626. ISSN 0037-1106.

[21] Gülerce Z, Kargıoğlu B., Abrahamson N.A., Turkey-Adjusted NGA-W1 Horizontal Ground Motion Prediction Models. Earthquake Spectra. 2016;32(1):75-100. doi: 10.1193/022714EQS034M

[22] Hisada, Y., and J. Bielak (2003). A theoretical method for computing near-fault ground motions in layered half-space considering static offset due to surface faulting, with a physical interpretation of fling step and rupture directivity, Bull. Seismol. Soc. Am. 93, no. 3, 1154–1168.

[23] Akbaş B., Tetik T., Önder F.M., Sopacı E., Tanırcan G., Ozacar A.A., and Gulerce Z. (2023). The New Turkish Strong Motion Dataset (N-TSMD) for earthquake engineering applications. Submitted to Bulletin of Earthquake Engineering

[24] International Conference of Building Officials (2006). International Building Code, Whittier, CA.

[25] International Conference of Building Officials (2007). California Building Code, Whittier, CA.

[26] American Society of Civil Engineers (2005), ASCE-7 Minimum Design Loads for Buildings, Reston, VA.